Eur Biophys J (2002) 31: 62–72
DOI 10.1007/s00249-001-0190-2

ARTICLE

Tomohiro Hayakawa · Mitsuhiro Hirai

Hydration and thermal reversibility of glycolipids depending on sugar chains

Received: 2 May 2001 / Revised version: 3 September 2001 / Accepted: 3 September 2001 / Published online: 9 November 2001

Abstract To elucidate a relationship between the structural properties and hydration characteristic of gangliosides, time-resolved small-angle X-ray scattering measurements using synchrotron radiation have been performed on aqueous dispersions of various types of gangliosides (G_{M1}, G_{D1a}, G_{D1b} and G_{M3}) under a constant heating (5–65 °C) and cooling (65–5 °C) rate. In the case of G_{M3}, they formed a vesicular aggregate with a high structural reversibility in the heating-and-cooling process. For the micelles of G_{M1}, G_{D1a} and G_{D1b}, we found an evident thermal hysteresis in the structural changes of their headgroups and evaluated quantitatively the amounts of water molecules occluded in the micellar hydrophilic regions by using the shell modeling method reported previously. For all cases of G_{M1}, G_{D1a} and G_{D1b}, the thickness of the hydrophilic region of the micelle shrunk after the heating process, and stayed mostly constant over the entire cooling range. On the other hand, the amounts of water molecules and the behavior of the G_{M1}, G_{D1a} and G_{D1b} micelles in the heating-and-cooling process greatly depended on the number of sialic acid residues in the sugar chain, that is, the penetration of water molecules was much more reversible for the G_{M1} micelle compared with those for the G_{D1a} and G_{D1b} micelles. The observed clear hysteresis and the hydration characteristics of G_{D1} gangliosides would relate to their role in neuronal membranes, where G_{D1} gangliosides show the greatest concentrations.

Keywords Hydration · Thermal structural transition · Micelle · Glycosphingolipid · Synchrotron radiation

T. Hayakawa · M. Hirai (✉)
Department of Physics,
Gunma University, 4-2 Aramaki,
Maebashi 371-8510, Japan
E-mail: mhirai@fs.aramaki.gunma-u.ac.jp
Tel.: +81-27-2207554
Fax: +81-27-2207551

Introduction

Gangliosides, glycosphingolipids containing sialic acid residues, locate mainly on the outer surfaces of cell membranes and are abundant in the tissues of the central nervous system (Ledeen and Yu 1982). Recently, these molecules have been reported to be enriched in lipid microdomains with other particular lipids and proteins in neuronal cells (Prinetti et al. 2000). Although studies of the role of gangliosides in the microdomains are limited (Kasahara et al. 2000), it is expected that the surfaces of the microdomains are highly hydrophilic due to an enrichment by the oligosaccharides of gangliosides, and complex networks of hydrogen bonding would be formed between water molecules and those lipid headgroups. Actually, it has been reported that a considerable number of water molecules is associated with the polar headgroup of gangliosides (Bach et al. 1982a; Arnulphi et al. 1997). The numbers of tightly bound unfreezable water molecules of gangliosides, estimated from calorimetric experiments by Bach et al. (1982b), are 22–30 for G_{M1}, 33–40 for a G_{D1a} and G_{D1b} mixture, and about 60 for a G_{T1b} and G_{Q1b} mixture. Moreover, besides the unfreezable water molecules above, the existence was reported of a large amount of loosely bound water molecules with a rotational correlation time ranging from 10^{-11} to 10^{-10} s (Arnulphi et al. 1997). The estimated numbers of these loosely bound water molecules are about five times larger than those of the tightly bound ones.

Such hydrophilic environments of ganglioside-enriched membrane would modulate the structure and dynamics of proteins associated in the microdomains and would affect the interactions between substrates and membranes. Maggio et al. (1994) and Daniele et al. (1996) showed that gangliosides have inhibitory effects on phospholipase A_2 and C activities. As phospholipase activity is concurrent with a dehydration process of the membrane interface (Jain et al. 1988), it is suggested that the high capacity of ganglioside for structural water plays a major role in these inhibitory effects (Arnulphi et al. 1997).

Thus it is particularly interesting to investigate the relationship between the dynamic properties of hydrated water and the structural characteristics of gangliosides. By using neutron and X-ray scattering techniques and calorimetry, we have reported the structural characteristics of ganglioside micelles depending on temperature (Hirai et al. 1996a, 1996b, 1998a, 1999; Hirai and Takizawa 1998), pH and concentration (Hirai et al. 1996b). We have also clarified the binding specificity of gangliosides with proteins depending on both oligosaccharide chain and protein surface modification (Hirai et al. 1995a, 1998b). We have shown the following results on the thermal structural stability of ganglioside micelles. The elevation of temperature induces a significant shrinkage of the hydrophilic region of the ganglioside micelle at physiological temperatures around 20–40 °C, indicating that the oligosaccharide chains of ganglioside molecules change those conformations sensitively against the rise of temperature (Hirai et al. 1996a, 1996b, 1998a). We also reported that this phenomenon accompanies the extrusion of a large amount of water from the hydrophilic region of the micelles (Hirai and Takizawa 1998) and an alteration of the micellar surface charge (Hirai et al. 1999). Moreover, a thermal hysteresis was observed in the behavior of the ganglioside G_{M1} headgroup between the first and second heating scans (Hirai et al. 1996a).

In the present study, we performed time-resolved synchrotron radiation small-angle X-ray scattering (SR-SAXS) measurements on various types of ganglioside (G_{M1}, G_{M3}, G_{D1a} and G_{D1b}) dispersions under a constant heating (5–65 °C) and cooling (65–5 °C) rate, aiming to obtain detailed features of the following: (1) behavior of the water molecules occluded within the hydrophilic regions of the ganglioside micelles, depending on the headgroup and temperature, (2) heat-induced structural changes of ganglioside headgroups, and (3) thermal hysteresis properties depending on ganglioside headgroups. High statistical scattering data from the synchrotron radiation made it possible to evaluate the intramicellar structure by using the well-defined shell-modeling analysis (Hirai et al. 1994, 1995a, 1995b, 1995c, 1996a, 1996b, 1996c, 1998a, 1998b, 1999; Hirai and Takizawa 1998). In this report, we show a distinct thermal hysteresis property of G_{D1} (G_{D1a} and G_{D1b}) gangliosides accompanied by irreversible water extrusion. In addition, previous evidence of a thermal hysteresis property for the G_{M1} ganglioside micelle (Hirai et al. 1996a) has been clearly confirmed.

Materials and methods

Ganglioside samples

The samples used were monosialoganglioside G_{M1} and disialoganglioside (G_{D1a}, G_{D1b}) from bovine brain and G_{M3} from canine blood, all purchased from Sigma (USA) and used without further purification. Each of the ganglioside powders with 0.5% w/v was dissolved in 50 mM Hepes [*N*-(2-hydroxymethyl)piperazine-*N*′-(2-ethanesulfonic acid)] buffer adjusted to pH 7.0 and used for the scattering experiments.

Small-angle X-ray scattering measurements

Small-angle X-ray scattering experiments were performed by using the synchrotron radiation small-angle X-ray scattering spectrometer installed at the BL10C line of the 2.5 GeV storage ring at the Photon Factory, High Energy Accelerator Research Organization, Tsukuba, Japan. The X-ray wavelength and the sample-to-detector distance were 1.49 Å and 87 cm, respectively. Time-resolved measurements were carried out on a programmed time-interval setting with the 55-s exposure time for each timeframe. After keeping the sample at ~5 °C overnight, the heating run was started from 5 to 65 °C at a heating rate of 1 °C/min. The cooling run was performed from 65 to 5 °C at a cooling rate of 1 °C/min after annealing the sample at 65 °C for 10 min.

Shell-modeling analysis

Above their critical micelle concentration (CMC), gangliosides (G_{M1}, G_{D1a} and G_{D1b}) are known to form ellipsoidal (prolate) micelles in an aqueous solution (Gammack 1963; Hirai et al. 1995a, 1995b, 1995c, 1996a, 1996b, 1996c, 1998a, 1998b, 1999; Hirai and Takizawa 1998). The following equation was applied for the profile fittings of the experimental scattering curves to estimate the structural parameters of the ganglioside ellipsoidal micelles:

$$I(q) = \int_0^1 \left[3\left(\bar{\rho}_1 V_1 \frac{j_1(qR_1)}{qR_1} + \sum_{i=2}^{n} (\bar{\rho}_i - \bar{\rho}_{i-1}) V_i \frac{j_i(qR_i)}{qR_i} \right) \right]^2 \mathrm{d}x \qquad (1)$$

where $I(q)$ is the spherically averaged scattering function of a particle with an ellipsoidal shape of revolution composed of n shells with different average excess scattering densities $\bar{\rho}_i$ (so-called contrast), i is the number of the shell and j_i is the spherical Bessel function of the first rank; R_i is defined as:

$$R_i = r_i\left(1 + x^2\left(v_i^2 - 1\right)\right)^{1/2} \qquad (2)$$

where r_i and v_i are the radius and semiaxial ratio of the ith ellipsoidal shell, respectively. $\bar{\rho}_i$, r_i and v_i were used as fitting parameters.

Evaluation of water within the micelle

As reported previously (Hirai and Takizawa 1998), we can evaluate the number n_w of water molecules occluded in the hydrophilic shell region by using the following equation based on the values of the structural parameters obtained from the shell-modeling analysis:

$$n_w = \left[\left\{ \frac{\Delta_{shell}}{\Delta_{core}} \left(\frac{\sum_{cer} b}{V_{cer}} - \alpha \right) + \alpha \right\} V_{shell} - n_a \sum\nolimits_{head} b \right] \Big/ \sum\nolimits_{water} b \qquad (3)$$

The definitions of the parameters used in the above equation are as follows. $\sum_{water} b$, $\sum_{head} b$, $\sum_{cer} b$, V_{water}, V_{head} and V_{cer} are the total scattering amplitudes and the excluded volumes of water molecules, the head and tail portions of the ganglioside molecule, respectively; $\alpha = \sum_{water} b / V_{water} = 9.4 \times 10^{10}$ cm^{-2}. As we know the chemical components of the water molecule, G_{M1} head, G_{D1} head and ceramide, we can calculate $\sum_{water} b = 2.81 \times 10^{-12}$ cm, $\sum_{head} b = 1.50 \times 10^{-10}$ cm for the G_{M1} head and 1.92×10^{-10} cm for the GD_1 head, $\sum_{cer} b / V_{cer} = 8.69 \times 10^{10}$ cm^{-2}. n_a is the aggregation number of ganglioside micelles estimated by $n_a = V_{core}/V_{cer}$; $\Delta_{shell}/\Delta_{core}$ is the ratio between the shell and core contrasts, which are obtained from the structural parameters of the shell-modeling analysis.

Results and discussion

Temperature dependence of the scattering curves

In previous studies on ganglioside dispersions using differential scanning calorimetry (DSC), the measurements were performed at a scan rate of around 0.5–10 °C/min (Sillerud et al. 1979; Hinz et al. 1981; Bach et al. 1982a; Maggio et al. 1985; Reed and Shipley 1996). As far as we know, no scan rate influences were observed in this range. We employed the heating-and-cooling rate of 1 °C/min for the present measurements, which is a common scan rate for DSC measurements on lipids.

Figure 1 shows the stability of the micellar structures of gangliosides after sample preparations. We confirmed that the scattering profile from the G_{M1} ganglioside solution does not show any change for at least three months, suggesting that the ganglioside micellar particle is quite stable. Other types of gangliosides also showed similar stability. Figure 2a–c shows the temperature dependence of the scattering curves of the G_{M1}, G_{D1a} and G_{D1b} micelles in the heating (5–65 °C) and cooling (65–5 °C) processes. The significant decrease of the scattering intensity below $q = 0.015$ Å^{-1} is caused by the presence of a beam-stopper. Every scattering curve has a minimum at $q = \sim 0.06$ Å^{-1} and a rounded peak at $q = \sim 0.1$ Å^{-1}, reflecting the globular micellar structure. In the heating processes (5–65 °C) of all samples shown in Fig. 2a–c, we can see the following three common features in the changing manners of the scattering profiles. Firstly, with the rise of temperature, the scattering intensities in the small-angle scattering region ($q < \sim 0.05$ Å^{-1}) decrease gradually, indicating that the average overall radii of the particles become smaller. Secondly, the rounded peak becomes broad for G_{D1}, and shifts slightly to the higher angle region for G_{M1}. Thirdly, the minima of the scattering curves stay at the same q position ($q = \sim 0.06$ Å^{-1}) over the entire heating range. In addition, for all samples the variations of the scattering patterns occur rather rapidly at the temperature range from 30 to 50 °C.

The scattering curves in the cooling process (65–5 °C) are also shown in Fig. 2a–c. The changing manners of the scattering curves in the cooling processes are different from those in the heating processes. Several points should be noted as the common features in the changing manners of the scattering profiles. Firstly, although the scattering curves at $q = 0.015$–0.06 Å^{-1} and the minimum positions ($q = \sim 0.06$ Å^{-1}) shift slightly to the higher-angle region with lowering temperature, the slopes of the

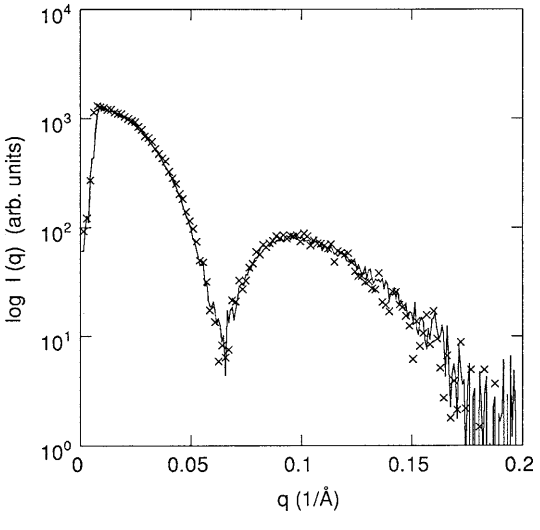

Fig. 1 Stability of scattering curves $I(q)$ from G_{M1} micelles. Scattering curves obtained at 24 h (*continuous line*) and 3 months (*crosses*) after sample preparation. For the 3 months results, the sample was kept at ~5 °C

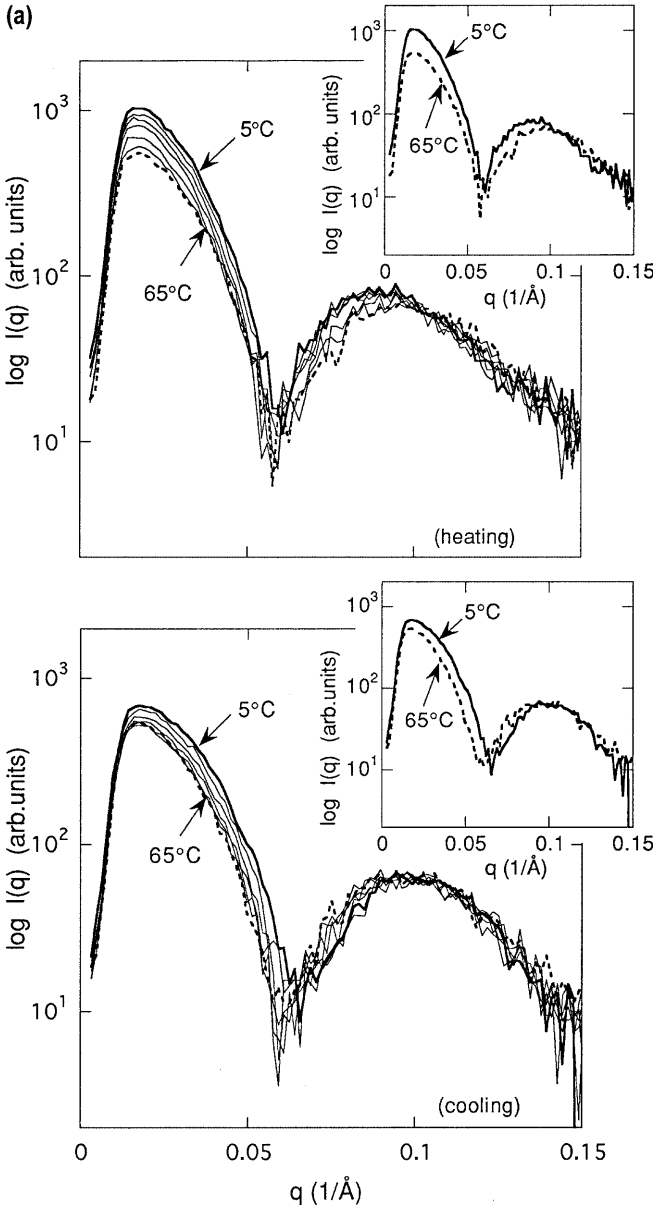

Fig. 2 Scattering curves $I(q)$ of G_{M1} (**a**), G_{D1a} (**b**) and G_{D1b} (**c**), depending on temperature variation under the constant heating and cooling rate of 1 °C/min. Scattering curves at 10 °C intervals are plotted in the temperature range from 5 to 65 °C

scattering curves in this q region show no major change. Secondly, the q positions of the rounded peaks ($q = \sim 0.1$ Å^{-1}) shift slightly to the higher-angle region. Thirdly, the slopes of the scattering curves at $q = 0.10$–0.13 Å^{-1} remain mostly constant. Comparing the characteristics of the changing manners of the scattering curves between the heating and cooling processes, evidently the thermotropic structural changes of the micelles take place in a different way between these two processes. In other words, the thermotropic structural changes of the ganglioside micelles have properties of thermal hysteresis under the present conditions. As shown in Fig. 3, such a hysteresis is not seen in the scattering patterns from G_{M3} aggregates, though G_{M3} gangliosides form vesicles in aqueous solutions (Sonnino et al. 1990; Maurer et al. 1995). In Fig. 3, with raising temperature, the scattering intensity in the small-angle region decreases, and the positions of the minimum ($q = \sim 0.05$ Å^{-1}) and the rounded peak ($q = \sim 0.08$ Å^{-1}) shift to the higher-angle region. These changes in the scattering profiles indicate that the average size of the G_{M3} aggregates becomes smaller, which is well reversible against the variation of temperature. This suggests that the observed hysteresis of the structural changes of the G_{M1} and G_{D1} micelles would be mainly attributed to their sugar-chain length and structure.

Micellar structures of gangliosides and shell-modeling analyses

The structural properties of the ganglioside aggregates in aqueous dispersions were investigated by Gammack

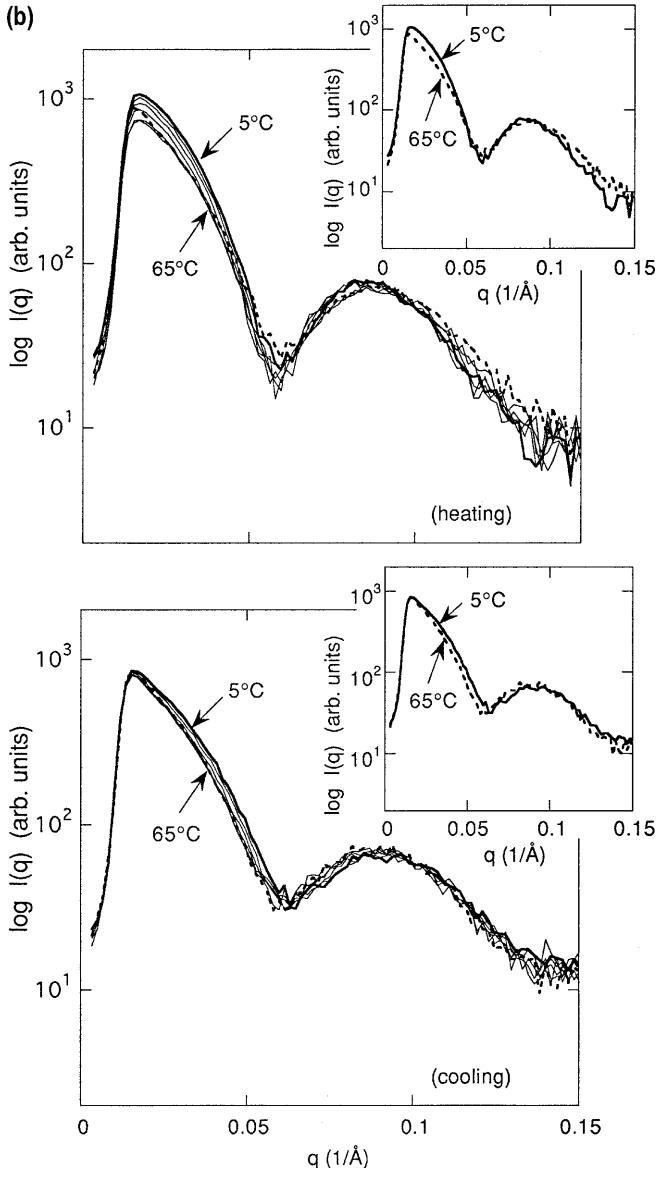

Fig. 2 (Contd.)

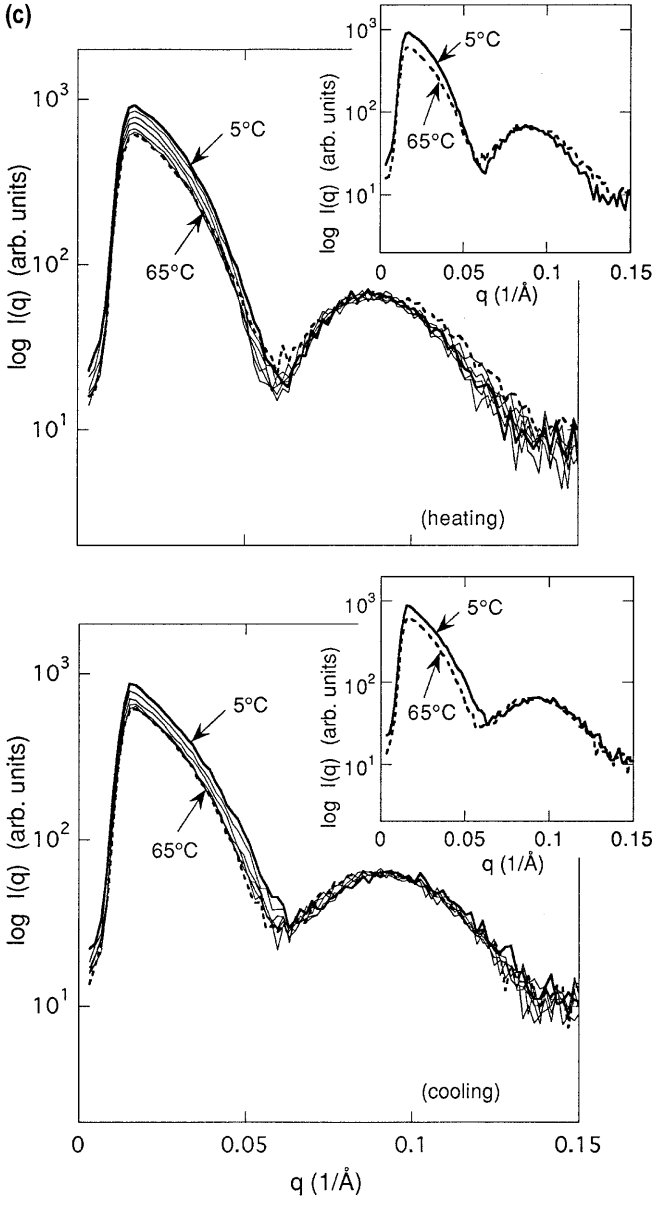

Fig. 2 (Contd.)

in early 1960s, who suggested that mixed ox-brain gangliosides form prolate ellipsoidal micelles, by means of sedimentation, diffusion and viscosity measurements (Gammack 1963). Hirai et al. later showed that not only mixed ganglioside but also pure G_{M1} and G_{D1a} ganglioside micelles are prolate in shape, by using small-angle X-ray and neutron techniques and the shell-modeling analysis (Hirai et al. 1995b, 1996a, 1996b, 1996c, 1998a, 1999; Hirai and Takizawa 1998). At low water content, Curatolo et al. (1977) revealed by calorimetric and X-ray diffraction measurements that mixed brain gangliosides exhibit a hexagonal mesophase structure (H_I), and Arnulphi et al. (1997) also confirmed the H_I structure in their study using ^2H NMR. As well described by Glatter (1982), a prolate ellipsoidal particle and an oblate one give quite different scattering curves $I(q)$ and distance distribution functions $p(r)$. Those differences are easily distinguishable by plotting $I(q)$ in a log scale. Figure 4a shows that the scattering curve $I(q)$ of the ganglioside G_{M1} micelle can be well simulated by the theoretical curve derived from a prolate double-shell ellipsoid model (Hirai et al. 1996a, 1998a; Hirai and Takizawa 1998) as described in Materials and methods. The definitions of the structural parameters used for the

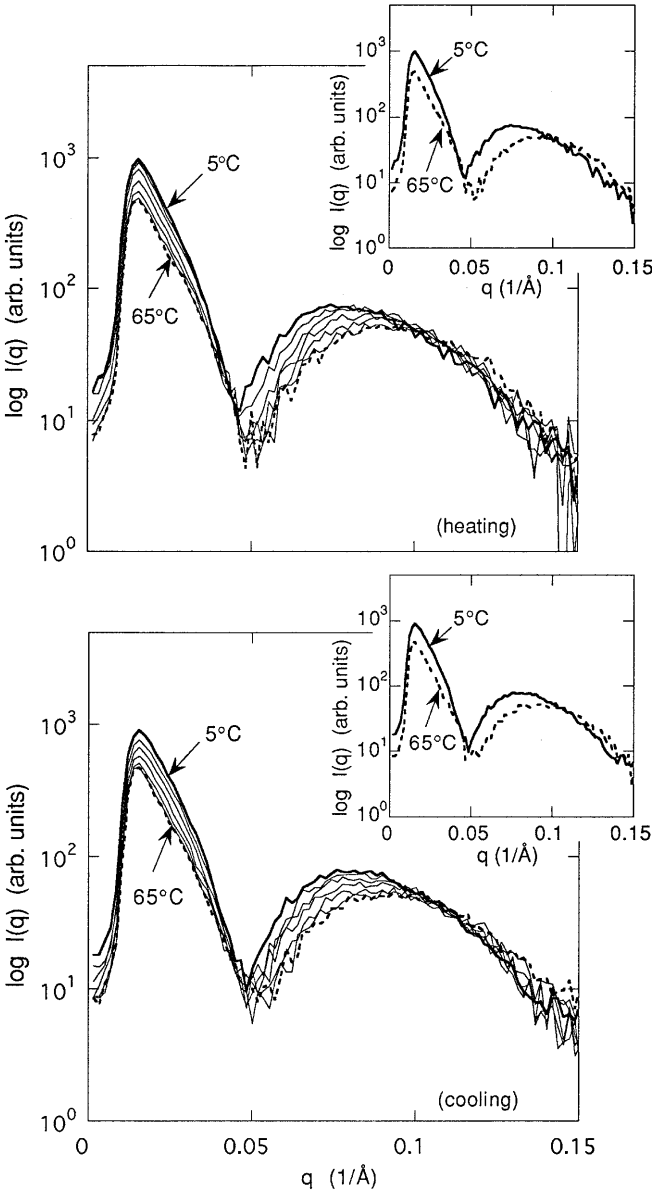

Fig. 3 Reversibility of scattering curves $I(q)$ from G_{M3} aggregates under a constant heating and cooling rate of 1 °C/min. Scattering curves at 10°C intervalls are plotted in the temperature range from 5 to 65°C. *Full lines* and *dashed lines* are curves in the heating and cooling processes, respectively

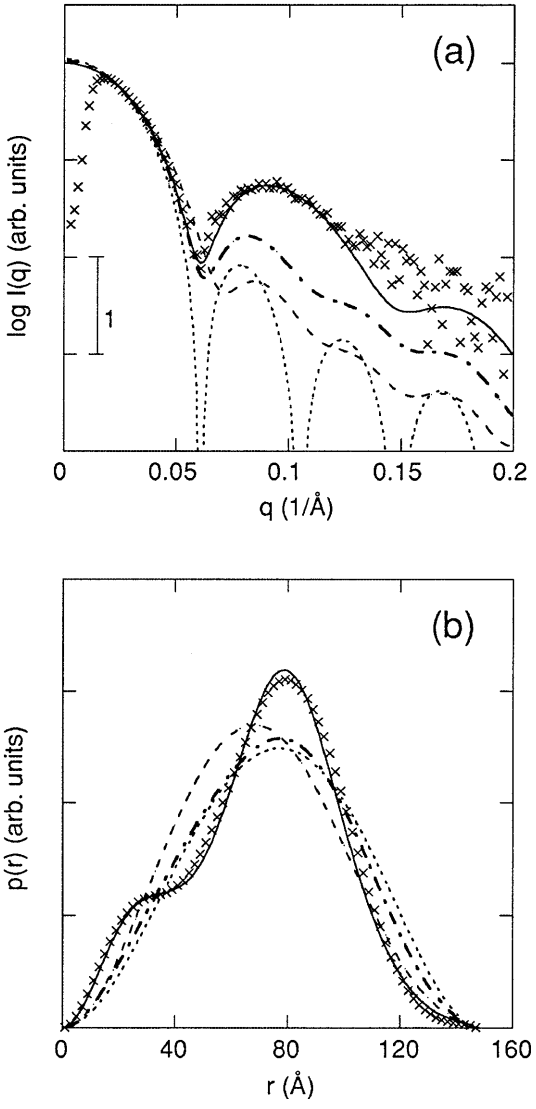

Fig. 4 Scattering curves $I(q)$ and distance distribution functions $p(r)$ from the model structures optimized to fit to the experimental data: **a** $I(q)$, **b** $p(r)$. In **a** and **b**, *crosses* represents the experimental $I(q)$ and $p(r)$ from the G_{M1} micelle at 5 °C in the heating process in Fig. 2a. The lines in Fig. 4 are the $I(q)$ and $p(r)$ for the different types of the model structures: *continuous line* for a double-shell prolate ellipsoid model; *dotted line* for a sphere model; *dashed line* for an oblate ellipsoid model; *dash-dot line* for a double-shell oblate ellipsoid model

present curve fittings and those obtained values at 5 °C in the heating run are shown in Fig. 5. The shell and core radii of the obtained model give reasonable values for the ganglioside chemical structure, that is, 24.5 Å for the hydrophilic headgroup and 27 Å for the hydrophobic ceramide moiety. Figure 4b shows the distance distribution function $p(r)$ obtained by the Fourier inversion of the $I(q)$ in Fig. 4a. The $p(r)$ profile of the theoretical model is in good agreement with that from the experiment. The obtained maximum dimension of the particle is 147 Å. As shown in Fig. 4a and b, other models having a 147 Å maximum dimension, that is, a simple sphere, an oblate ellipsoid with a homogeneous scattering density, or a double-shell oblate ellipsoid, do not fit the experimental data, indicating a high sensitivity of SR-SAXS data to those intramolecular structures.

To obtain quantitative information on the internal structure of the ganglioside micelles, a shell-modeling analysis was performed by the procedure described previously (Hirai et al. 1994, 1995b, 1996a, 1996b, 1996c, 1998a, 1999; Hirai and Takizawa 1998). As shown in Fig. 6, the experimental scattering curves of the G_{M1}, G_{D1a} and G_{D1b} micelles are well simulated by the theoretical curves derived from Eq. (1). Especially, the curves in the q region of 0.02–0.03 $Å^{-1}$, which mainly represent the size and shape of the solute particles, are in excellent agreement, indicating a high reasonability of the employed model fittings and a high monodispersity of the sample solutions. Because of the simplified double-shell models with smooth surfaces, the theoretical scattering curves in the higher scattering-angle region ($q > 0.13$ $Å^{-1}$) show some disagreement with the experimental ones. However, the model fittings of the experimental scattering curves by a simple sphere or ellipsoid having a homogeneous electron density show much worse agreement with the theoretical ones in the higher scattering-angle region, as we described elsewhere (Hirai et al. 1996b).

In Fig. 7, the shell and core radii of the ganglioside micelles obtained from the model fittings are plotted against temperature. The initial values of the shell radii of the G_{M1}, G_{D1a} and G_{D1b} micelles at 5 °C are 51.5, 53.5 and 52.0 Å, respectively. In the heating process from ~20 to ~55 °C, the shell radius of the G_{M1} micelle decreases gradually to the value of 45.7 Å, and it shows no major change above ~55 °C. The G_{D1a} and G_{D1b} micelles mostly maintain the shell radii at temperatures from 5 to 30 °C. Above 30 °C, the shell radii of the G_{D1a} and G_{D1b} micelles decrease gradually and continuously to the value at 65 °C of 46.8 Å for G_{D1a}, and 45.9 Å for G_{D1b}. On the other hand, the shell axial ratios of all samples shown in Fig. 8 are mostly stable through the temperature cycle, in spite of a slight increase seen in the heating process. In the cooling process, the structures of all samples show irreversible behavior to the temperature variation. The shell radii of the G_{D1a} and G_{D1b} micelles stay virtually constant at those values at 65 °C all the way to 5 °C, whereas the shell radius of the G_{M1}

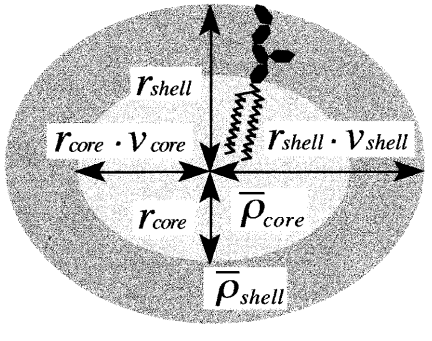

Fig. 5 Schematic structure of prolate ganglioside micelle. r_{shell}, r_{core}, ν_{shell}, ν_{core}, $\bar{\rho}_{shell}$ and $\bar{\rho}_{core}$ are the shell and core radii, the shell and core axial ratios, and the relative values of scattering density (contrast) for the shell and core, respectively. For example, those values obtained fromz the model fitting at 5 °C in the heating process are 51.5 Å and 27 Å, 1.4 and 1.7, 0.54 and –0.4, respectively

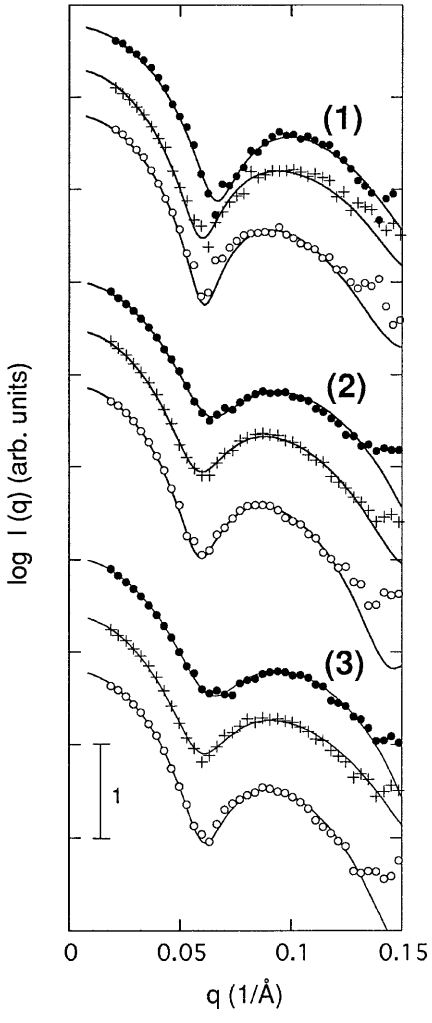

Fig. 6 Scattering curves $I(q)$ from the model structures optimized for the experimental data of G_{M1} (*1*), G_{D1a} (*2*) and G_{D1b} (*3*). For each sample, 5 °C heating (*1*), 65 °C (*2*), 5 °C cooling (*3*), *full lines* represent theoretical scattering curves fitted to the respective experimental data

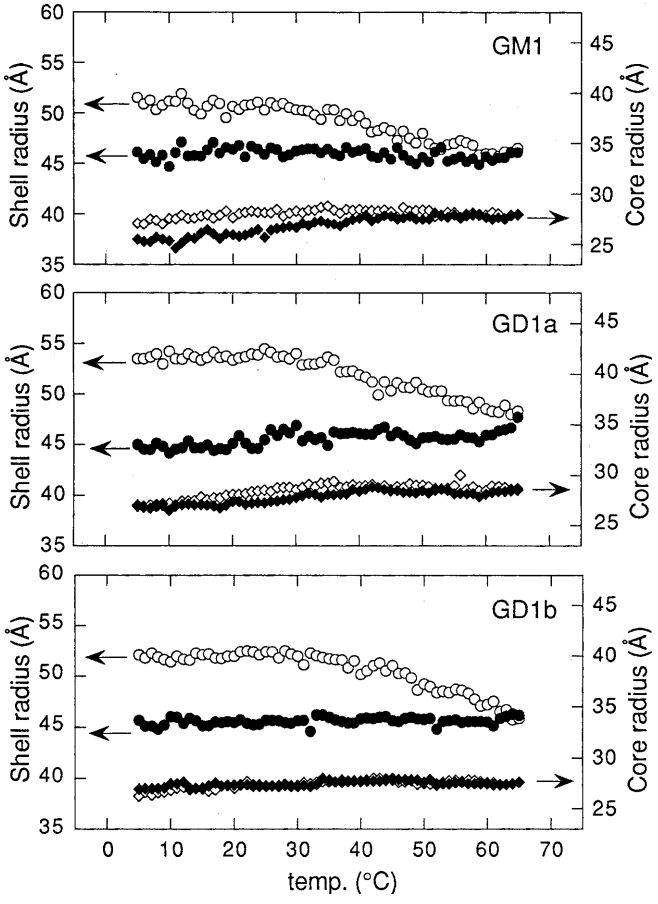

Fig. 7 Shell and core radii of the ganglioside micelle estimated by the shell-modeling analysis, plotted against temperature. *Circles* are used for shell radii, *diamonds* for core radii. *Open* and *full symbols* represent the values in the heating and cooling processes, respectively

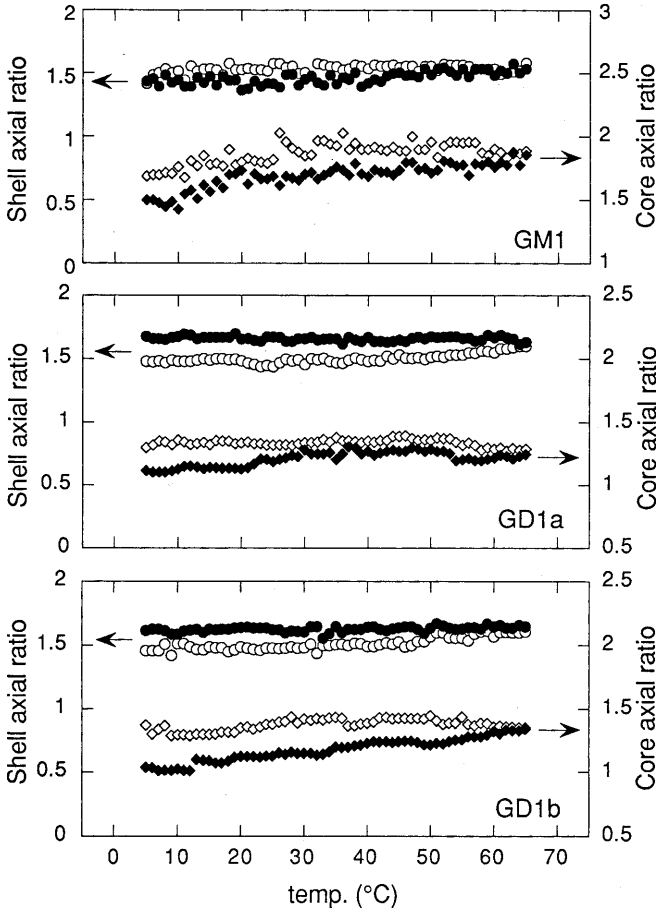

Fig. 8 Shell and core axial ratios of the ganglioside micelle estimated by the shell-modeling analysis, plotted against temperature. *Circles* are used for shell axial ratios, *diamonds* for core axial ratios. *Open* and *full symbols* are as in Fig. 4

micelle shows a slight recovery. The final values of the shell radii of the G_{M1}, G_{D1a} and G_{D1b} micelles at 5 °C are 46.2, 45.0 and 45.7 Å, respectively. The axial ratios of the G_{D1a} and G_{D1b} micelles in the cooling process are mostly constant against the temperature variation, whereas the G_{M1} axial ratio decreases to the initial value in the heating process.

Compared with the case of the shell radius, the core radius of each sample shows no major change throughout the entire heating range. Slight expansions and contractions with temperature variation are observed for all samples. For example, the core radius of the G_{M1} micelle is 27.0 Å at 5 °C in the heating run and increases to 28.8 Å at 35 °C, then decreases to 27.9 Å at 65 °C. This core behavior could be considered a result of some heat-induced rearrangement of the hydrocarbon chains in the micelles (Curatolo et al. 1977; Masserini and Freire 1986), since no sharp peaks of endothermal transitions were detected in many DSC studies on ganglioside micelles (Sillerud et al. 1979; Hinz et al. 1981; Masserini and Freire 1986; Reed and Shipley 1996). Also, a recent study of GM1 ganglioside micelles using Fourier transform infrared spectroscopy (FT-IR) clearly indicates that GM1 micelles do not show a thermal phase transition in the temperature range 5–60 °C (Khalil et al. 2000). The reported volume ratios of CH_2 and CH_3 groups between L_β (gel) and L_α (fluid) phases are 25.5 $Å^3$/27.0 $Å^3$ and 51.0 $Å^3$/54.0 $Å^3$, respectively (Marsh 1990). Therefore, even if the slight expansion and contraction of the core radius seen in Fig. 4 could be an effect of the L_β-L_α type transition, the expected volume change by this phase transition would be about 6%. Then, in this study, the estimated changes in the relative contrast between 5 °C and 65 °C are ~2% for all samples analyzed. However, the changes of the core and shell radii observed in this study may correspond to the broad endothermic peaks in DSC studies of ganglioside dilute solutions. For example, Bach et al. (1982a) obtained endothermic peaks in the range 10–48 °C for ~20% w/v G_{M1} in Tris-HCl buffer with 0.15 M NaCl. They also reported that they observed similar peaks in the same temperature range for a ~2% w/v G_{M1} sample. Reed and Shipley (1996) also observed a broad endothermic peak from 5 to 40 °C with a peak maximum at 23.5 °C for ~0.58% w/v G_{M1} in phosphate buffer.

The above structural behavior of the shell and core regions, together with the slight increase of the shell contrasts in the heating process shown in Fig. 9, directly indicate that the oligosaccharide portions of the ganglioside molecules in the micelles become contracted by the temperature elevation. Furthermore, by the present shell-modeling analyses, the irreversible profiles of the scattering curves shown in Fig. 2 can be interpreted as a sugar-chain-dependent hysteresis of the structural change of the ganglioside molecules.

Evaluation of water molecules in the micellar hydrophilic region

It was clarified previously that a considerable amount of tightly and loosely bound water molecules are associated with the headgroups of gangliosides (Bach et al. 1982a; Arnulphi et al. 1997). The recent Laurdan fluorescence measurements of ganglioside micelles (Bagatolli et al. 1997, 1998) also showed that generalized polarization (GP) values of G_{M1} and G_{D1a} ganglioside aggregates maintain those of liquid crystalline phases in the temperature range 2–45 °C for G_{M1} and 4–28 °C for G_{D1a}. These results suggest that the hydrophilic-hydrophobic interfaces of ganglioside micelles are rich in water in those temperature ranges. However, the behavior of water molecules of G_{M1}, G_{D1a} and G_{D1b} micelles above those temperatures, where hysteresis of structural changes of ganglioside headgroups would mainly occur, are still obscure.

To clarify the behavior of water molecules within the shell region of ganglioside micelles under the present condition, we have estimated the number n_w of water molecules per ganglioside headgroup in the micelles based on the scheme described in Materials and methods. Figure 10 shows the relationship of the n_w value versus temperature for the G_{M1}, G_{D1a} and G_{D1b} micelles. G_{D1} gangliosides contain much larger amounts of water molecules than G_{M1}, that is, the estimated n_w values at 5 °C in the heating process are about 130 for G_{M1}, 220 for G_{D1a}, and 200 for G_{D1b}. These values show a great reproducibility of this analysis when compared to our previous results (Hirai and Takizawa 1998). In this

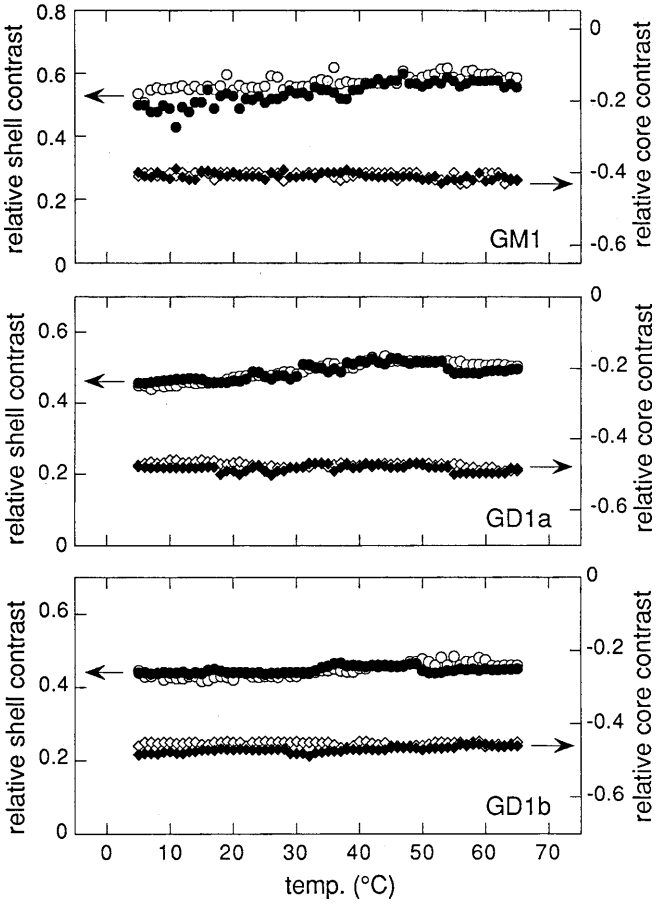

Fig. 9 Shell and core contrasts of the ganglioside micelle estimated by the shell-modeling analysis, plotted against temperature. *Circles* are used for shell contrasts, *diamonds* for core contrasts. *Open* and *full symbols* are as in Fig. 4

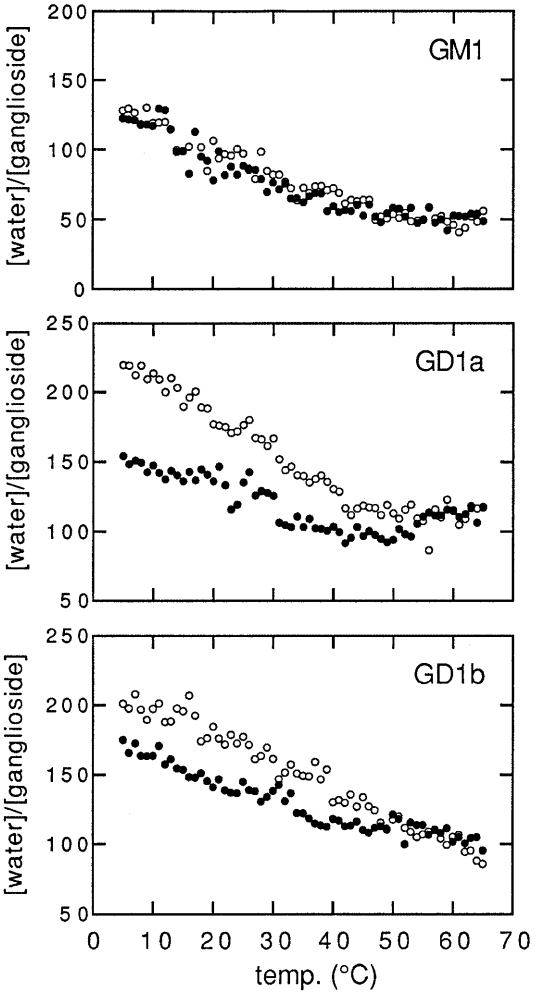

Fig. 10 Temperature dependence of the number of water molecules per ganglioside molecule occluded in the micelle. *Open* and *full symbols* are as in Fig. 4

analysis, we cannot distinguish between bound water and simply occluded "free" water in the hydrophilic region of the ganglioside micelle. However, these n_w values would represent mostly the numbers of water molecules bound to the headgroups in some manner, since the ^2H NMR experiments and analyses (Arnulphi et al. 1997) indicate that all water molecules in the [water]/[total brain ganglioside] = 200/1 system at a micellar phase can be assigned to tightly and loosely bound ones having correlation times of 2×10^{-9} s and 6×10^{-10} s, respectively. Therefore, the numbers of water molecules estimated in the present analyses contain mostly both tightly and loosely bound ones, and the amount of "free" water molecules which have a correlation time on the order of 10^{-12} s, if they exist, would be quite small.

For each ganglioside micelle, the values of n_w in the shell regions start to decrease immediately with the rise of temperature, and 40–50 water molecules are excluded prior to the structural change of ganglioside headgroups at ~20–30 °C. This suggests that the loosely bound water that is sensitive to temperature has a role in the structural stability of the headgroups. For the G_{M1} case in the heating process, the value of n_w decreases linearly to a value of about 50 at 65 °C. The n_w value of G_{D1a} decreases rapidly to a value of about 120 with the rise of temperature from 5 to 40 °C. Above 40 °C, the n_w value of G_{D1a} shows no major variation until 65 °C. On the other hand, the n_w value of G_{D1b} decreases gradually and linearly to a value of about 90 at 65 °C. According to previous calorimetric experiments (Bach et al. 1982a), the number of unfreezing water molecules associated with a ganglioside headgroup is about 22–30 for G_{M1} and 33–40 for G_{D1} ($G_{D1a} + G_{D1b}$). Also, 30 water molecules on average were found to be tightly bound to a headgroup of a bovine brain ganglioside mixture, as shown in the ^2H NMR experiments (Arnulphi et al. 1997). Therefore, the lowest n_w value at 65 °C for each ganglioside in the present analysis would contain not only tightly bound water but also loosely bound water and simply occluded water.

The behavior of water in the shell regions of the ganglioside micelles are considerably different between G_{M1} and G_{D1} in terms of thermal reversibility. In the cooling process, the n_w value of G_{M1} increases linearly and rather reversibly to about 120 at 5 °C, whereas the n_w values of G_{D1a} and G_{D1b} do not show such a reversibility. The final value of n_w of G_{D1a} at 5 °C in the cooling process is about 150. On the other hand, the n_w value of G_{D1b} shows a relatively reversible behavior compared with that of G_{D1a}, namely, the n_w value of G_{D1b} at 5 °C in the cooling process is about 170. These differences of the water behavior or the n_w values between the ganglioside species could be attributable to the structural characteristics of ganglioside molecules, namely, to the number and attached position of the sialic acid residues and the structural flexibility of the headgroup. Moreover, these hydration properties of G_{M1} and G_{D1} would relate to the headgroup-dependent inhibitory effect of gangliosides on phospholipase C activity, shown by Daniele et al. (1996). However, owing to the observed hysteresis behavior of G_{D1} and its water molecules, the interactions between G_{D1} and substrates may be altered in the case that G_{D1} is well heat-treated before measurements.

Conclusion

In the present work, we investigated the details of the relationship between the structure of ganglioside headgroups and the behavior of water molecules in the micellar hydrophilic region under a constant heating-and-cooling rate. We observed clearly the hysteresis of the structural changes of the G_{D1a} and G_{D1b} micelles accompanied by irreversible water occlusion. Also the previous evidence of a thermal hysteresis property of the G_{M1} ganglioside micellar structure (Hirai et al. 1996a, 1998a) with reversible water occlusion has been clearly confirmed. Once contracted, the oligosaccharide portion of the G_{M1} and G_{D1} micelles in the heating process did not show a reversible behavior in the temperature cycle (Fig. 6). These irreversible conformational changes of the sugar chains would restrict the water penetration into the hydrophilic region of the micelles in the cooling process. The observed difference between the hysteresis behavior of G_{M1} and G_{D1} is likely due to the difference between their headgroup flexibilities or abilities to form intra- and/or intermolecular hydrogen bonds. Namely, the G_{M1} and G_{D1} molecules have additional N-H and C=O groups in their oligosaccharide moieties which can be involved in the formation of intra- and intermolecular hydrogen bonds (Boggs 1987; Scarsdale et al. 1990). Actually, the dispersions of G_{M3} molecules which would not form intramolecular hydrogen bonds, due to their conformational restrictions, did not show hysteresis behavior under the same experimental conditions (Fig. 3). Water molecules occluded in the micellar shell regions for all samples decreased with the rise of temperature (Fig. 10). This phenomenon would give a better opportunity to form transient hydrogen bonds for the oligosaccharide moieties of gangliosides. On the other hand, in the cooling process, water molecules were occluded again reversibly for the G_{M1} micelle, whereas water molecules in the shell region of G_{D1a} and G_{D1b} micelles showed relatively irreversible behavior, corresponding to the conformational changes of their headgroups. In the temperature range measured, loosely bound or "free" water molecules were observed more or less in the shell region for each micelle, which is consistent with the fluorescence experimental results of Bagatolli et al. (1997, 1998). As described in Results and discussion, we cannot distinguish between hydrated water and "free" water in the hydrophilic region of micelles by the present analysis. Therefore, it would be still ambiguous on the behavior of tightly bound water molecules and their contribution to the structural stability of oligosaccharide chains of gangliosides.

Other physicochemical factors or some agents in vivo, which lead to the dehydration of gangliosides, may also cause a similar hysteresis characteristic of ganglioside aggregates as shown in this report. These properties of gangliosides would affect and/or modulate membrane fluidity, topology, surface membrane hydration characteristics and activities of proteins associated with ganglioside-enriched membranes. Our recent study of the dynamics of ganglioside micelles using the neutron spin echo (NSE) technique suggests that the dehydration and bending of the ganglioside sugar chains with elevating temperature reduce the deformation motion of the micelle, namely that the dynamics of the micelle is coupled with the conformational state of ganglioside headgroups (Hirai et al. 2001). Furthermore, as both the conformational change of gangliosides and the behavior of water molecules in the shell region alter the micellar surface charge (Hirai et al. 1999), not only lateral organization of gangliosides in cell membranes but also the state of ganglioside headgroups themselves might be one of the major determinants for cell-cell interaction or cell-protein interaction.

Acknowledgements We thank Mr. Iwase of Gunma University for his help with the small-angle X-ray scattering measurements. This work was performed under the approval of the Photon Factory Program Advisory Committee (proposal no. 98G185) of the High Energy Accelerator Research Organization (KEK), Tsukuba, Japan.

References

Arnulphi C, Levstein PR, Ramia ME, Martin CA, Fidelio GD (1997) Ganglioside hydration study by ^{2}H-NMR: dependence on temperature and water/lipid ratio. J Lipid Res 38:1412–1420

Bach D, Miller IR, Sela B-A (1982a) Calorimetric studies on various gangliosides and ganglioside-lipid interactions. Biochim Biophys Acta 686:233–239

Bach D, Sela B, Miller IR (1982b) Compositional aspects of lipid hydration. Chem Phys Lipids 31:381–394

Bagatolli LA, Maggio B, Aguilar F, Sotomayor CP, Fidelio GD (1997) Laurdan properties in glycosphingolipid-phospholipid mixtures: a comparative fluorescence and calorimetric study. Biochim Biophys Acta 1325:80–90

Bagatolli LA, Gratton E, Fidelio GD (1998) Water dynamics in glycosphingolipid aggregates studied by Laurdan fluorescence. Biophys J 75:331–341

Boggs JM (1987) Lipid intermolecular hydrogen bonding: influence on structural organization and membrane function. Biochim Biophys Acta 906:353–404

Curatolo W, Small D, Shipley GG (1977) Phase behavior and structural characteristics of hydrated bovine brain gangliosides. Biochim Biophys Acta 468:11–20

Daniele JJ, Maggio B, Bianco ID, Goni FM, Alonso A, Fidelio GD (1996) Inhibition by gangliosides of *Bacillus* phospholipase C activity against monolayers, micelles and bilayer vesicles. Eur J Biochem 239:105–110

Gammack DB (1963) Physicochemical properties of ox-brain gangliosides. Biochem J 88:373–383

Glatter O (1982) Data treatment. In: Glatter O, Kratky O (eds) Small-angle X-ray scattering. Academic Press, London, pp 119–196

Hinz HJ, Korner O, Nicolau C (1981) Influence of ganglioside G_{M1} and G_{D1a} on structural and thermotropic properties of sonicated small 1,2-dipalmitoyl-L-α-phosphatidylcholine vesicles. Biochim Biophys Acta 643:557–571

Hirai M, Takizawa T (1998) Intensive extrusion and occlusion of water in ganglioside micelles with thermal reversibility. Biophys J 74:3010–3014

Hirai M, Hirai T, Ueki T (1994) Growing process of scattering density fluctuation of a medium distance in the hydrogel of poly(vinyl alcohol) under stretching. Macromolecules 27:1003–1006

Hirai M, Takizawa T, Yabuki S, Nakata Y, Mitomo H, Hirai T, Shimizu S, Furusaka M, Kobayashi K, Hayashi K (1995a) Complexes of gangliosides with proteins in solution. Physica B 213/214:751–753

Hirai M, Yabuki S, Takizawa T, Nakata Y, Mitomo H, Hirai T, Shimizu S, Kobayashi K, Furusaka M, Hayashi K (1995b) Ganglioside structure in solution. Physica B 213/214:748–750

Hirai M, Hirai RK, Yabuki S, Takizawa T, Hirai T, Kobayashi K, Amemiya Y, Oya M (1995c) Aerosol-OT reversed micellar formation at low water-surfactant ratio studied by synchrotron radiation small-angle X-ray scattering. J Phys Chem 99:6652–6660

Hirai M, Takizawa T, Yabuki S, Nakata Y, Hayashi K (1996a) Thremotropic phase behavior and stability of monosialoganglioside micelles in aqueous solution. Biophys J 70:1761–1768

Hirai M, Takizawa T, Yabuki S, Hirai T, Hayashi K (1996b) Thermotropic structural change of disialoganglioside micelles studied by using synchrotron radiation small-angle X-ray scattering. J Phys Chem 100:11675–11680

Hirai M, Takizawa T, Yabuki S, Hayashi K (1996c) Intermicellar interaction of ganglioside aggregates and structural stability on pH variation. J Chem Soc Faraday Trans 92:4533–4540

Hirai M, Arai S, Takizawa T, Yabuki S, Nakata Y (1998a) Characteristics of thermotropic phase transition of glycosphingolipid (ganglioside) aggregates in aqueous solution. Thermochim Acta 308:93–99

Hirai M, Iwase H, Arai S, Takizawa T, Hayashi K (1998c) Interaction of gangliosides with proteins depending on oligosaccharide chain and protein surface modification. Biophys J 74:1380–1387

Hirai M, Iwase H, Hayakawa T (1999) Thermal induced modulation of surface charge of sialoglycosphingolipid micelles. J Phys Chem B 103:10136–10142

Hirai M, Iwase H, Hayakawa T (2001) Structure and dynamics of glycosphingolipid micelles. J Phys Soc Jpn 70:420–423

Jain MK, Rogers J, DeHaas GH (1988) Kinetics of binding of phospholipase A_2 to lipid/water interfaces and its relationship to interfacial activation. Biochim Biophys Acta 940:51–62

Kasahara K, Watanabe K, Takeuchi K, Kaneko H, Oohira A, Yamamoto T, Sanai Y (2000) Involvement of gangliosides in glycosylphosphatidylinositol-anchored neuronal cell adhesion molecule TAG-1 signaling in lipid rafts. J Biol Chem 275:34701–34709

Khalil MB, Kates M, Carrier D (2000) FTIR study of the monosialoganglioside G_{M1} in perdeuterated dimyristoylglycerophosphocholine ($DMPC_{d54}$) multilamellar bilayers: spectroscopic evidence of a significant interaction between Ca^{2+} ions and the sialic acid moiety of G_{M1}. Biochemistry 39:2980–2988

Ledeen RW, Yu RK (1982) Gangliosides: structure, isolation, and analysis. Methods Enzymol 83:139–191

Maggio B, Ariga T, Sturtevant JM, Yu RK (1985) Thermotropic behavior of glycosphingolipids in aqueous dispersions. Biochemistry 24:1084–1092

Maggio B, Bianco ID, Montich GG, Fidelio GD, Yu RK (1994) Regulation by gangliosides and sulfatides of phospholipase A2 activity against dipalmitoyl- and dilauroylphosphatidylcholine in small unilamellar bilayer vesicles and mixed monolayers. Biochim Biophys Acta 1190:137–148

Marsh D (ed) (1990) Dilatometric data. In: CRC handbook of lipid bilayers. CRC Press, Boca Raton, pp 185–194

Masserini M, Freire E (1986) Thermotropic characterization of phosphatidylcholine vesicles containing ganglioside G_{M1} with

homogeneous ceramide chain length. Biochemistry 25:1043–1049

Maurer N, Cantu L, Glatter O (1995) Physicochemical behavior of the ganglioside G_{M3} in dilute aqueous solutions. Chem Phys Lipids 78:47–54

Prinetti A, Chigorno V, Tettamanti G, Sonnino S (2000) Sphingolipid-enriched membrane domains from rat cerebellar granule cells differentiated in culture. J Biol Chem 275:11658–11665

Reed RA, Shipley GG (1996) Properties of ganglioside G_{M1} in phosphatidylcholine bilayer membranes. Biophys J 70:1363–1372

Scarsdale JN, Prestegard JH, Yu RK (1990) NMR and computational studies of interactions between remote residue gangliosides. Biochemistry 29:9843–9855

Sillerud LO, Schafer DE, Yu RK, Konigsberg WH (1979) Calorimetric properties of mixtures of ganglioside G_{M1} and dipalmitoylphosphatidylcholine. J Biol Chem 254:10876–10880

Sonnino S, Cantu L, Acquotti D, Corti M, Tettamanti G (1990) Aggregation properties of G_{M3} ganglioside (II^3Neu5AcLacCer) in aqueous solutions. Chem Phys Lipids 52:231–241